Available online www.jsaer.com

***Journal of Scientific and Engineering Research*, 2017, 4(7):230-242**

Research Article

ISSN: 2394-2630
CODEN(USA): JSERBR

Response Surface Methodology for Stabilized Turbulent Confined Jet Diffusion Flames Using Bluff-Body Burners

Tahani S. Gendy, Amal S. Zakhary, T. M. El-Shiekh

Egyptian Petroleum Research Institute (EPRI), Nasr City, Cairo, Egypt

Abstract The Response Surface Methodology (RSM) has been applied to investigate the thermal structure of stabilized confined jet diffusion flames in the presence of different geometries of bluff-body burners. Two stabilizer disc burners tapered at 30° and 60° and another frusted cone of 60°/30° inclination angle were employed all having the same diameter of 80 (mm) acting as flame holders. The measured radial mean temperature profiles of the developed stabilized flames at different normalized axial distances (x/d_j) were considered as the model example of the physical process.

The RSM analyzes the effect of the two operating parameters namely (r), the radial distance from the center line of the flame, and (x/d_j) on the measured temperature of the flames and to find the predicted maximum and the corresponding process variables. Also it has been employed to illustrate such effects in the three and two dimensions and shows the location of the predicted maximum temperature.

Keywords Turbulent flames, bluff-body burners, thermal structure, mathematical modeling, response surface methodology

Introduction

Turbulent diffusion flames are usually used in industrial applications to improve the efficiency of practical burners. The co-axial jet diffusion flames enhance the flame by using flame holder such as bluff-bodies to generate a recirculation zone in which the fuel and oxidizer mix thoroughly. The flow features was influenced by the different shapes of bluff-bodies creating a large scale motion of the re-circulated vortices, prolong stagnation of reactants which is a key factor to flame stabilization regime [1-2]. Moreover, with the increase in lip thickness of bluff-body geometry, the flame length gets reduced, increasing the flame temperature and enhancing flame stability [3-4].

Quantification of the duration of the blow-off event, for unconfined lean premixed methane–air flames stabilized on an axisymmetric bluff body, showed that it was an order of magnitude longer than the characteristic timescale of the bluff body diameter d/U_b, where U_b is the bulk velocity at the annular passage [5]. Investigating the effect of flame holder geometry on flame structure shows that increasing in the flame holder length or its radius decreases flame length and increases flame temperature. Additionally, it is observed that the flame temperature is higher for smaller flame lengths [6].

Recently, turbulent non-premixed flames of natural gas and air stabilized in a semi-infinite bluff-body burner were assessed either to jet or to wake dominated the base of flow fields to identify the influence of the fuel jet and air coflow velocities on the measured results [7]. The velocity fields' was analyzed under score of the local extinctions and the interactions between combustion and turbulence. Reynolds stresses distribution comparison reveals that the flame presence generates turbulence in intermittently lifted situations and suppresses part of the Reynolds stresses when fully lifted.

The present study focuses on the analyses through mathematical modeling the previously reported experimental data of thermal structure of the stabilized flames in the presence of different geometries of bluff-body burners

[8]. The **RSM** has been utilized to study the effect of two different operating parameters, namely the namely the radius and **(x/d_j)** on the mean radial temperature profiles of the developed stabilized flames. Also **RSM** has been is employed to illustrate such effects in the three and two dimensions and shows the location of the predicted optimum maximum temperature for the investigated three bluff-body burners.

Experimental

Details of the experimental setup and the data employed in this study have been given the previous work of [8-9].

Response Surface Methodology

RSM is an assembly of mathematical and statistical techniques that are useful for the modeling and analysis of problems in which a response of interest is influenced by several variables and the objective is to optimize this response [10]. Experimentation is made to determine the effect of the independent variables (factors) on the dependent variable say response of a process and a relation between them is usually demonstrated through a regression model by using experimental data and optimization methods [11-13]. By means of it, it is possible to locate the optimum conditions and to analyze how sensitive the optimum conditions are to variations in the settings of the experimental variables. It also provides graphic illustrations of the shape of the surfaces, thus allowing a visual interpretation of the functional relations between the response and the experimental variables [14].

In general, if all variables are assumed to be measurable, the relationship between the response y and independent variables $\xi_1, \xi_2, \dots, \xi_k$ is [14]:

$$y = f\left(\xi_1, \xi_2, \dots, \xi_k\right) + \varepsilon \qquad (1)$$

Where the form of the true response function f is unknown and perhaps very complicated, so we must approximate it and ε is a term that represents other sources of variability not accounted for in f. The variables $\xi_1, \xi_2, \dots, \xi_k$ in Equation (1) are usually called the natural variables. The units of the natural independent variables differ from one another, besides not all of these variables will be tested over the same range.In much RSM work it is convenient to transform the natural variables ξ_i to coded variables $X_1, X_2, \dots, X_k$, which are usually defined to be dimensionless in the domain of [-1,1] with mean zero and the same standard deviation. Commonly used equation for coding is seen below [15-16].

$$coded\ value = \frac{actual\ value - mean}{half\ of\ range}$$

Usually, a low-order polynomial first-order or second-order model is appropriate [14]. The relation-ship between the coded variables and the response is modeled, in this work, by adjusting the experimental data to a second-order polynomial according to the following equation:

$$Y = \beta_0 + \sum_{i=1}^{k} \beta_i X_i + \sum_{i=1}^{k} \beta_{ii} X_i^2 + \sum_{\substack{i=1 \\ i<j}}^{k-1} \sum_{j=2}^{k} \beta_{ij} X_i X_j + \varepsilon \qquad (2)$$

where, Y is the response variable; X_i and X_j are the input coded values of the variables that influence the response variable and ε represents the random error. k is the number of variables, and β_0, β_i, β_{ii} and β_{ij} are the regression coefficients of intercept, linear, quadratic and interaction terms, respectively [17]. This coded model is flexible and the factor coefficients immediately become comparable to one another, which serves for the scale-free ranking of the relative importance of the factors [18].

Ordinary Least Squares (OLS) method that minimizes the variance of the unbiased estimators of the coefficients is usually applied to estimate the coefficients of the equation. Insignificant coefficients for terms which did not influence the response were removed from the fitted model and then rerun the model without them. The final model should contain only significant parameters (with P-value <0.05) [19]. To guarantee that the equation fits the data well we assess the adequacy of the "fitted" equation through the following indicators [20].

Regression Statistics

R^2: It is a measure of how well the regression equation approximates the real data. A good model fit should yield an R^2 of at least 0.8.

Adjusted R^2: An unbiased estimate of the coefficient of determination. It penalizes the statistic R^2 if unnecessary extra variables terms are included in the model.

F-value is used to evaluate the overall significance of the model, in which the calculated value of ***F*** should be greater than the ***F***-table value at a specific level of significance, **α-*value*** [21-22].

Regression Significance F: A significant relationship between the independent and dependent variables is considered to exist if this value **< α = 0.05**.

P-value of each coefficient and the Y-intercept less than 0.05 indicates that the corresponding variable has a significant effect on the response with a fit level of more than 95%. Coefficient with smaller ***p-value***or greater magnitude of **|t-value|**denotes more significance into the model equation [23].

Confidence Limits are the 95% probability that the true value of the coefficient lies between the 95% Lower and Upper values. The narrower this ranges the better.

Prediction Statistics

Predictive Error Sum of Squares (PRESS): It is a measure of how the model fits each point in the design andhow it is likely to predict the response in a new experiment. Small values are desirable [21].

Predicted R-Squared **(R^2_{pred}):**It is a measure of the amount of variation in prediction of new data explained by the model.$R^2_{pred}$and R^2_{adj} should be within 0.20 of each other [16, 21].

Adequate precision statistic(Adeqval) is used to measure the ratio of the signal to noise. A ratio greater than 4 is an indicator of adequate model differentiation and the model could be used to navigate the design space(Cochran & Cox, 1992).

Coefficient of Variation(CV) indicates the degree of precision with which experiments were performed. Values below 10% might be considered excellent [24].

Average absolute deviation (AAD) is an indication of the goodness of fit of the equation. The ***AAD*** is calculated by the following equation:

$$\mathbf{AAD} = \{[\sum_{i=1}^{n}(|y_{i,exp} - y_{i,cal}|/y_{i,exp})]/n\} * 100 \quad (3)$$

Where $y_{i,exp}$and $y_{i,cal}$are the experimental and calculated responses and n is the number of experimental runs [15].

Residuals analysis

Graphical residual analysis should be conducted to validate the assumptions involved in the **ANOVA** of a normal residuals distribution (the normal probability plot will resemble a straight line) and the variance is constant (plot of residuals vs. run time or the predicted response should be structureless) [15].

Application of RSM to the present work

The coded factors of (r) and (x/d_j)have been calculated employing the following formulas:

$$\mathbf{R} = r/75 \ , \qquad X = \frac{(x/d_j) - 136}{104} \quad (4)$$

Where:

r: radial distance from the center line of the flame(mm)

x **:**axial distance along the flame over the disc (mm)

d_j**:**jet diameter(mm)

Employing the second-order relationship (2) and the above formulas (4) the following equation for the ***coded factors*** has been applied for the present work:

$$Y = \beta_0 + \beta_1 * R + \beta_2 * X + \beta_{11} * R^2 + \beta_{22} * X^2 + \beta_{12} * R * X \quad (5)$$

Several mathematical models have been suggested to establish the relationship between dependent and independent variables. The Box-Cox method can be used to identify a suitable power transformation to the response data for normalizing the data or equalizing its variance [16, 22].

Box-Cox method (BC)

A suitable power transformation **λ** for the data is based on the relation: $Y^* = Y^{\lambda}E$.

λ is determined using the given data such thatSS_E is minimized (whereE is the error between the given experimental response values and its transformed ones).The following relation is used to obtainY^{λ} :

$$Y(\lambda) = \begin{cases} \frac{Y^{\lambda}-1}{\lambda}\frac{1}{g^{\lambda-1}}, & if\ \lambda \neq 0; \\ lnY \times g, & if\ \lambda = 0 \end{cases} \qquad (6)$$

Where g, is the geometric mean of the response vector. Once a value of Y^{λ} is obtained for a value of λ, the corresponding $SS_E$for this value is calculated. The process is repeated for a number of λ values to obtain a plot of SS_E against λ. The value of λ corresponding to the minimum SS_E is selected. This is performed by plotting the Ln (SS_E) values against λ values because the range of SS_Evalues is large. Then the 100 (1- α) percent confidence interval for the selected λ is calculated. If the limits for λ do not include the value of one, then the transformation is applicable for the given response data. For details of this method refer to [16].

This method has been utilized and the results are depicted in figs (1: a-c) and table (1). The following transformations; of the mean temperature T dependent variable; sqrt(T), Ln(T) and (T) have been employed for D30, D60 and DFC respectively to represent the response Y in equation(5).

Equation (5) has been applied to the experimental data cited in Ref [8]. The regression has been performed employing Microsoft Excel 2010 and Matlab 8.1 to determine the coefficients of the equation for the ***coded factors*** along with the statistical parameters depicted in **Table 2** which validate the results.

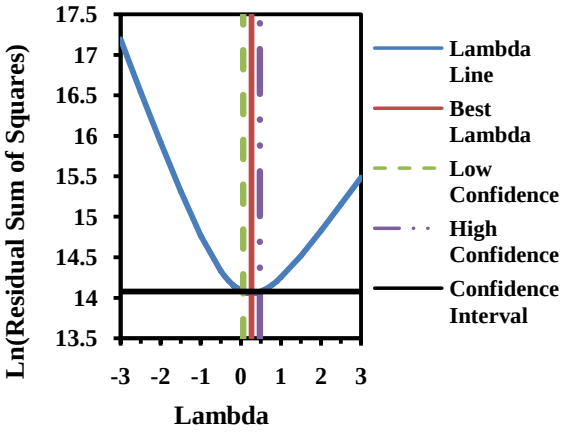

Figure (1-a): BOX COX Plot for D30

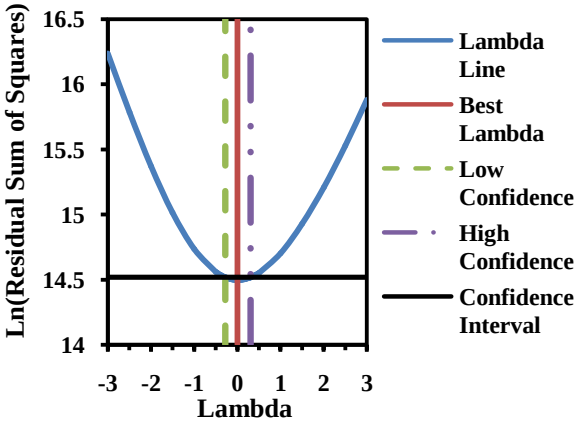

Figure (1-b): BOX COX Plot for D60

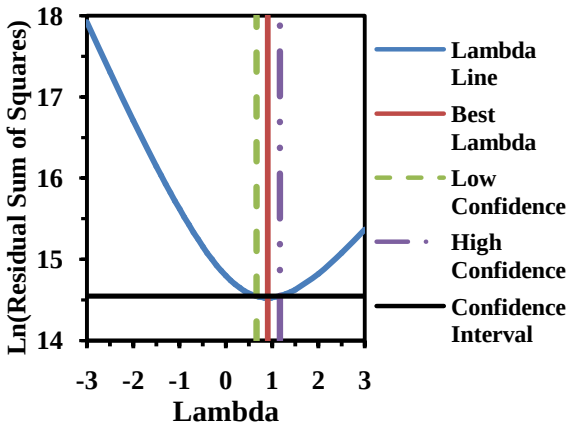

Figure (1-c): BOX COX Plot for DFC

Table 1: Values of BOX COX Plot

BOX COX Plot	**Disc**		
	Disc Tapered at 30°	***Disc Tapered at 60°***	***Frusted Cone at 60°/30°***
Risk Level α	0.05	0.05	0.05
Best Lambda	0.267	0.01	0.902
λ for Low Confidence	0.058	-0.278	0.663
λ for High Confidence	0.476	0.302	1.162
Ln(RSSE) for Confidence Interval	14.07	14.51	14.54

Table 2: Regression Statistics and Analysis of Variance for the Flame Stabilizing Disc Burners

			Discs		
			Disc Tapered at 30°	***Disc Tapered at 60°***	***Frusted Cone at 60°/30°***
Regression Statistics		**R^2**	**0.944**	**0.897**	**0.936**
		Adjusted R^2	**0.942**	**0.895**	**0.935**
		Standard Error	**1.146**	**0.121**	**76.11**
Analysis of Variance	**Regression**	**MS**	**989.5**	**4.476**	**5.01E+6**
		df	**4**	**5**	**3**
	Residual	**MS**	**1.314**	**0.015**	**5793.2**
		df	**180**	**176**	**178**
	F		**753.1**	**308.0**	**864.1**
	Significance F		**3.44E-111**	**5.02E-85**	**8.28E-106**
Prediction Regression Statistics	**PRESS**		**251.9**	**2.763**	**1.08E+06**
	R^2pred		**0.9399**	**0.889**	**0.9324**
	Adeqval		**106.3**	**65.72**	**106.8**
	CV		**3.85**	**1.831**	**7.16**
	Average Absolute Deviation %		**6.76**	**9.50**	**6.87**

Results and Discussions

In **Table 2** the high and close R^2_{adj} to the R^2 values insures the satisfactory adjustment of the model equations to the experimental data. The very high values of calculated ***F-value*** in addition to the very low values of Significance **F,** besides the very close agreement between the "R^2_{pred}" values with the corresponding "R^2_{adj}" ones designate that there is a real and good relation between the independent and dependent variables. The adequate precision values of (78-106) in this study indicate adequate models discrimination and each of these models could be used to navigate the design space .The low values of **PRESS** and ***CV***<10show the high precision and good reliability of the performed experiments. Finally the small **(AAD)** values support the adequacy of the employed equations. These results indicate that the developed equation models can be

employed for the prediction of the temperature profile for any new data for the factors x/d_j& r, within the investigated limits.

Table 3: Estimated Regression Parameters for the Flame Stabilizing Discs

$$Y = \beta_0 + \beta_1 * R + \beta_2 * X + \beta_1^2 * R^2 + \beta_2^2 * X^2 + \beta_{12} * R * X$$

Regression Parameters		*Disc Tapered at 30°*	*Disc Tapered at 60°*	*Frusted Cone at 60°/30°*
	Coeff.	35.242	6.957	1426.7
	± C.L.	0.3271	0.0343	-22.0423
β_0	Standard Error	0.166	0.017	11.170
	t Stat	212.6	400.7	127.7
	P-value	4.39E-218	1.78E-262	5.36E-177
	Coeff.	-1.012	-0.0089	
	± C.L.	0.3249	0.0351	
β_1	Standard Error	0.165	0.018	
	t Stat	-6.148	-0.5017	
	P-value	4.92E-09	6.16E-01	
	Coeff.	3.911	0.3165	205.05
	± C.L.	0.2498	0.0263	-16.85
β_2	Standard Error	0.127	0.013	8.537
	t Stat	30.90	23.75	24.02
	P-value	7.11E-74	8.75E-57	9.68E-58
	Coeff.	-12.159	-1.025	-840.1
	± C.L.	.5989	0.0642	-40.41
β_1^2	Standard Error	0.303	0.033	20.48
	t Stat	-40.06	-31.48	-40.03
	P-value	1.33E-91	3.30E-74	1.19E-92
	Coeff.	-4.043	-0.2023	-289.5
	± C.L.	0.4988	0.0520	-33.21
β_2^2	Standard Error	0.253	0.026	16.83
	t Stat	-15.99	-7.680	-17.20
	P-value	2.12E-36	1.06E-12	1.08E-39
	Coeff.		-0.0735	
	± C.L.		0.0524	
β_{12}	Standard Error		0.027	
	t Stat		2,766	
	P-value		6.28E-03	
Experimental Max. Temp.		1400	1275	1550
Predicted Max. Temp.		1311.1	1190.5	1463.0
% AD for Pred. Max. Temp.		6.35	6.63	5.61
r for Max. Pred. Temp.		-3.1	-2.4	-6.39E-06
$x/d_j$for Max. Pred. Temp.		186.3	218.0	172.8

Table 3 depicts the values of only the significant coefficients of the employed equation (5) along with the corresponding low values of **$p < (\alpha = 0.05)$**, small Standard Error, large ***t-Stat*** and small coefficients limits in comparison with their corresponding ones which mean that they do not span the zero as a value for the parameter. This ensures the reliability of established equations for prediction for new data. The empty cells belong to the eliminated non-significant coefficients. The positive sign in front of the model terms indicates synergistic effect while the negative sign indicates antagonistic effect.

For both discs tapered at 30°&60° the effect of axial distance along the flame over the disc (x/d_j) for the temperature variation of the flame is more pronounced than that of the radial distance from the center line of the flame(r). This is manifested in the smaller ***p-value*** and larger **|*t-stat*|** of $\boldsymbol{\beta_2(X)}$ than that of $\boldsymbol{\beta_1(R)}$ in addition to

the larger value of $|\boldsymbol{\beta_2}|$ than that of $|\boldsymbol{\beta_1}|$ in (table3) [18, 23]. Table (3) also indicates, for the disc tapered at 60°, the interaction effect of the axial distance along the flame **(x)** and the radial distance **(r)** over the variation of flame temperature as marked by the significant $\boldsymbol{\beta_{12}}$ **(RX)**. As for the frusted cone 60°/30°the effect of the radial distance is not distinct as declared by the insignificant $\boldsymbol{\beta_1}$ **(R)** and the significant $\boldsymbol{\beta_{11}}(\mathbf{R^2})$due to the change of geometry of this bluff-body.

The high ability of the various model equations to predict the response has been declared in high correlation between the experimental data and predicted values $(\mathbf{R^2 \geq 0.9})$ revealed in Fig. (2: a-c). The normal probability plots of the studentized residuals in Figs. 3(a–c) reveal that the residuals fall on a straight line implying that the errors are distributed normally. The structureless pattern in the plot of the studentized residuals versus run number and predicted response (Figs 4&5(a-c)) indicated that the equation models are adequate and they do not show any violation of the independence or constant variance assumptions involved in the **ANOVA.**

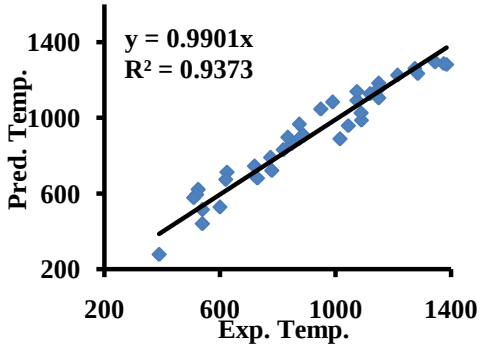

Figure (2-a): Predicted Temp. vs Experimental Temp for D30

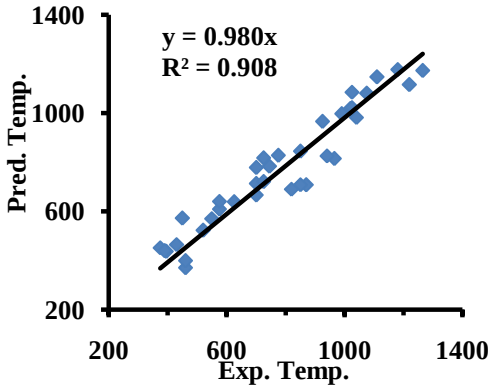

Figure (2-b): Predicted Temp. vs Experimental Temp. for D60

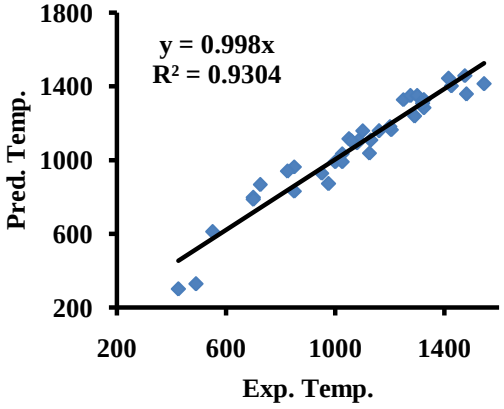

Figure (2-c): Predicted Temp. vs Experimental Temp. for DFC

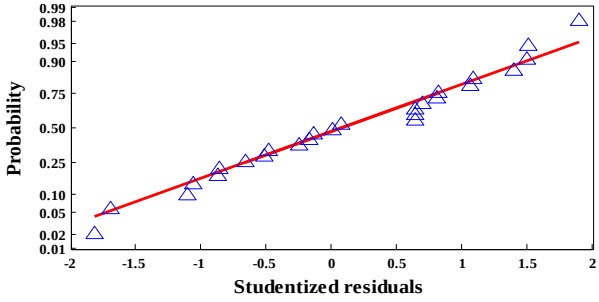

Figure (3-a): Normal plot of Studentized residuals for D30

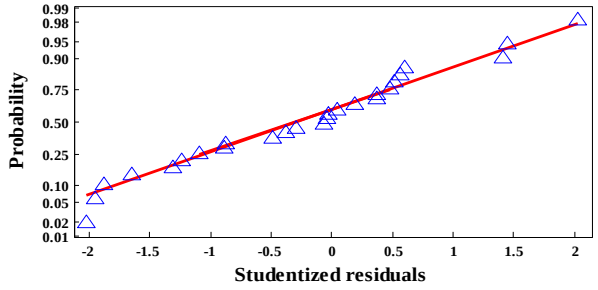

Figure (3-b): Normal plot of Studentized residuals for D60

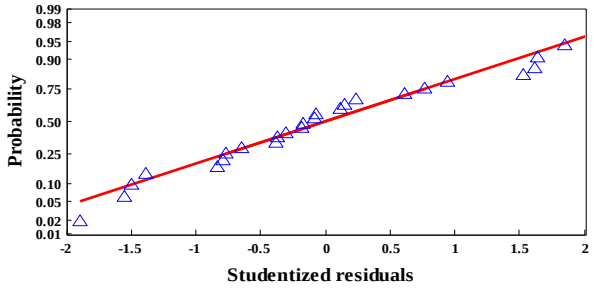

Figure (3-c): Normal plot of Studentized residuals for DFC

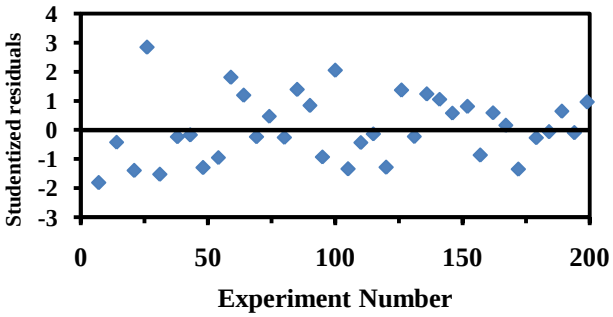

Figure (4-a): Studentized residuals vs Experiment Number for D30

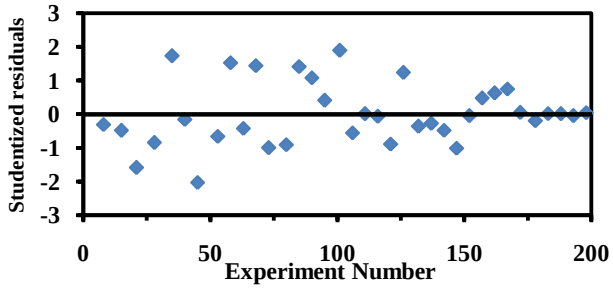

Figure (4-b): Studentized residuals vs Experiment Number for D60

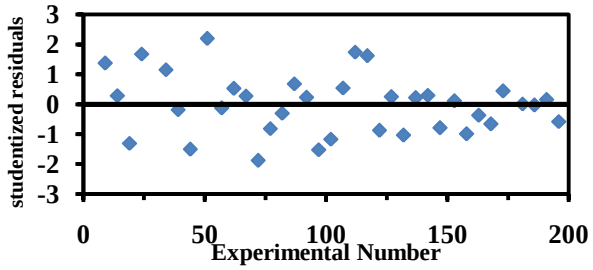

Figure (4-c): Studentized residuals vs Experiment Number for DFC

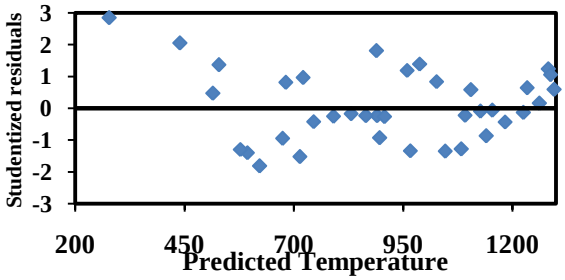

Figure (5-a): Studentized residuals vs Predicted Temperature for D30

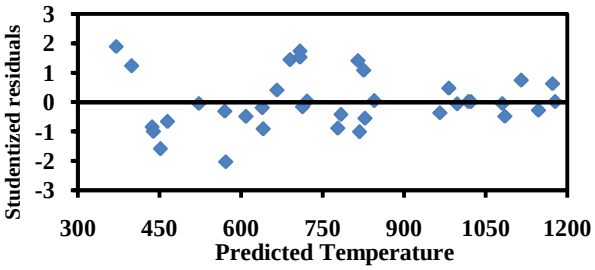

Figure (5-b): Studentized residuals vs Predicted Temperature for D60

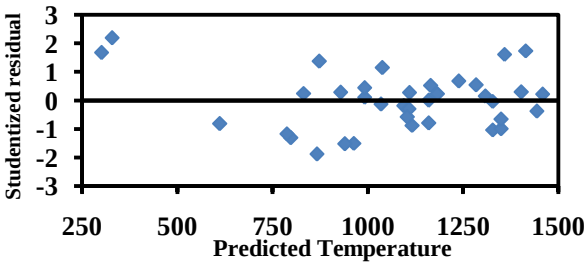

Figure (5-c): Studentized residuals vs Predicted Temperature for DFC

Equation Models in terms of natural factors:

The response relation with the natural independent variables has been investigatedemploying **(OLS)** method and it is represented by the following equations:

i- for D30

$$sqrt(T) = 23.21 - 1.35E-2 * r + 0.1393 * (x/d_j) - 2.162E-3 * r^2 - 3.738E-4 * (x/d_j)^2 \quad (7)$$

ii- for D60

$$Ln(T) = 6.197 + 1.163E-3 * r + 8.132E-3 * (x/d_j) - 1.822E-3 * r^2 - 1.871E-5 * (x/d_j)^2 - 9.423E-6 * r * (x/d_j) \quad (8)$$

iii- for DFC

$$T = 663.5 + 9.252 * (x/d_j) - 0.1494 * r^2 - 0.0268 * (x/d_j)^2 \quad (9)$$

Optimization

An optimization process has been performed, with the aid of Matlab8.1, for the above presented equations (7-9) to estimate the maximum predicted temperature and the corresponding ***r*** and **(x/d_j)** values for the various investigated cases. The Matlab performs a multidimensional unconstrained nonlinear optimization that uses the Nelder-Mead simplex (direct search) method.

These results are depicted in (table 3) together with the corresponding maximum experimental temperature. The small values of the % absolute deviation **(AD)< 10** for the predicted maximum from the corresponding maximum experimental values employing equation (3) supports the adequacy of the employed predictive equations.

The various developed equation models (7-9) have been employed, (utilizing Matlab 8.1), to display ***the Response Surface plots*** for the predicted temperatures versus the actual natural variables of (***r***) and **(x/d_j)** as illustrated in Figs (6: a-c) together with the corresponding experimental values. The maximum predicted responses are also shown in the response surface plots. Most of the experimental points fall on the predicted Response Surface which reflects the accuracy of the developed model equations. The two-dimensional Contour plots have been portrayed in Figs (7: a-c) along with the corresponding maximum predicted responses.

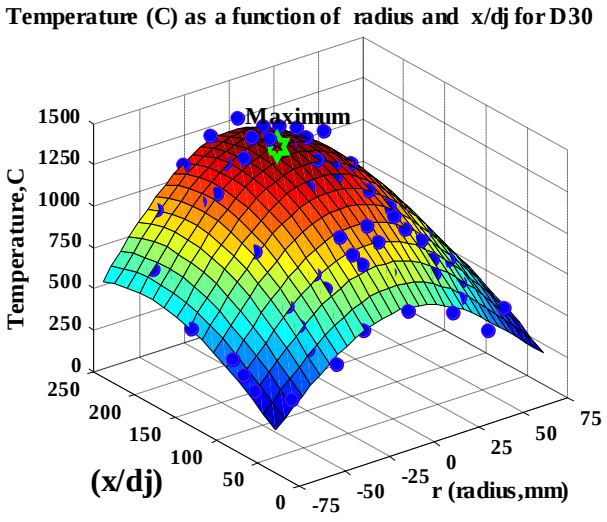

Figure (6-a): Surface plot for D30

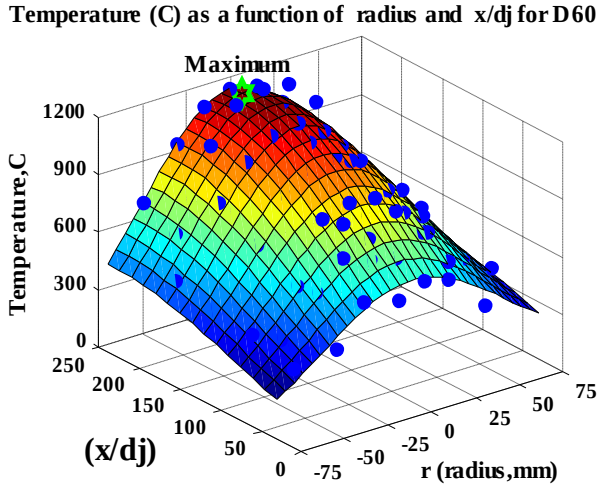

Figure (6-b): Surface plot for D60

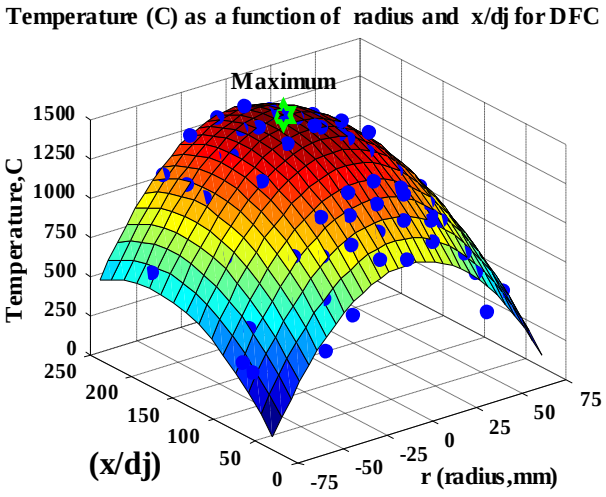

Figure (6-c): Surface plot for DFC

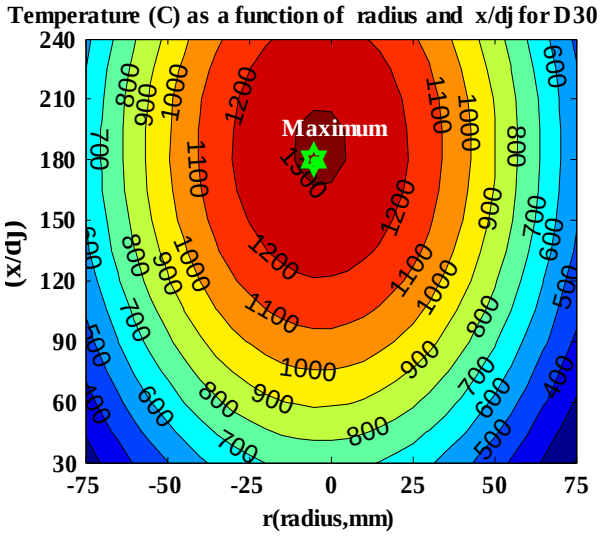

Figure (7-a): Contour plot for D30

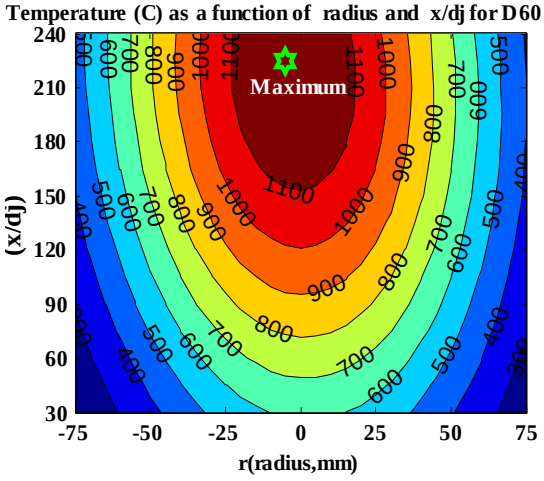

Figure (7-b): Contour plot for D60

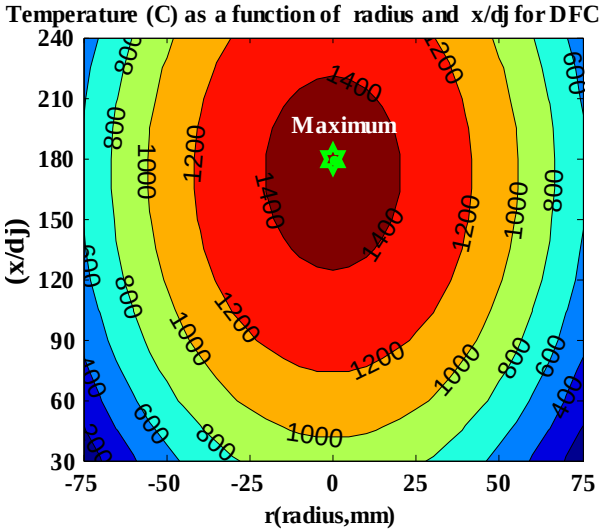

Figure (7-c): Contour plot for DFC

Conclusion

The response surface methodology (**RSM**) with the aid of Box-Cox method has been utilized to establish the suitable relations for the effect of radial distance **(*r*)** and normalized axial distance **(x/d_j)** on the thermal structure (T) of the flames in the presence of the various stabilizer discs. The developed least squares regression models showed excellent prediction for the experimental results with high values for $\mathbf{R^2}$ and $R^2_{adj} \geq$ **0.9**, high values of calculated ***F-value***, ***Adeqval***, and small values of significance **F** and ***AAD***. The models also presented good predictability for the response in a new experiment revealed in the small values of ***PRESS*** and high values of R^2_{pred}. The response surface illustrated in the three dimensions depicted the response of the predicted variable T to the variation of the studied variable parameters ***r*** & x/d_j with the good agreement between the experimental and predicted results and showed the location of the optimum maximum predicted temperature. The developed equation models can be employed for the prediction of the temperature profile for any new data for the factors x/d_j & r within the investigated limits.

References

[1]. Zakhary, A. S. 1990. *Study of a Stability and Structure of Confined Gaseous Turbulent Diffusion Flames.* Ph. D. Thesis Faculty of Engineering, Ain Shams University, Egypt.

[2]. Jing-Tang-Yang, Chia-Chi-Chang and Kuo-Long-Pan. 2002. Flow Structure and Mixing Mechanisms behind a Disc Stabilizer with a Central Fuel Jet. *Combustion Science and Technology*. 174:93-124.

[3]. Mishra, D. P. and Kiran D. Y. 2009.Experimental Studies of Bluff-Body Stabilized LPG.*Diffusion Flames.Fuel*. 88:573-578.

[4]. Navarro-Martinez, S. and Kronenburg, A. 2011. Flame Stabilization Mechanism in Lifted Flames.*Flow Turbulence Combust*. 87:377-406.

[5]. Kariuki, J, Dawson, J.R. and Mastorakos, E. 2012.Measurements in Turbulent Premixed Bluff-Body Flames Close to Blow-off.*Combustion and Flame.* 159:2589-2607.

[6]. Hashemi, S.A.,Hajialigol, N.,Fattahi, A.,Mazaheri, K. and Heydari, R. 2013.Investigation of a Flame Holder Geometry Effect on Flame Structure in Non-Premixed Combustion.*Journal of Mechanical Science and Technology*. 27:3505-3512.

[7]. Caetano, N.R. and da Silva, L.F.F. 2015. A Comparative Experimental Study of Turbulent Non-Premixed flames Stabilized by a Bluff-Body Burner. *Experimental Thermal and Fluid Science*. 63:20-33.

[8]. Zakhary, A. S. 2005. Thermal Structure of Stabilized Turbulent Confined Jet Diffusion Flames Using Bluff-Body Burners. *Scientific Bulletin, Faculty of Engineering, Ain Shams University, Egypt.* 40:751-763.

[9]. Gendy, T. S., El-Shiekh T.M. and Zakhary, A.S. 2015. A Polynomial Regression Model for Stabilized Turbulent Confined Jet Diffusion Flames Using Bluff Body Burners. *Egyptian Journal of Petroleum*.24:445-453.

[10]. Aslan, N. & Cebeci, Y.2007 .Application of Box–Behnken design and response surface methodology for modeling of some Turkish coals. *Fuel.* 86:90–97.

[11]. Raissi, S. 2009. Developing New Processes and Optimizing Performance Using Response Surface Methodology. *World Academy of Science, Engineering and Technology.* 25:1039-1042.

[12]. Gendy T. S., El-Temtamy S. A.,Ghoneim S. A., El-Salamony R. A., El-Naggar A. Y. and El-Morsi A. K. 2016. Response Surface Methodology for Carbon Dioxide Reforming of Natural Gas.*Energy Sources, Part A: Recovery, Utilization, and Environmental Effects*.38:1236–1245.

[13]. Gendy, T., Elsalamony, R.,Ghoneim, S, Mohamed, L., Ebiad, M. and Abd El Hafiza, D. 2014. Numerical Evaluation and Analysis for Hydrogen Production Via Ethanol Steam Reforming. *Chemical and Process Engineering Research*. 21:107-117.

[14]. Carley M. K.,Kamneva N. Y. &Reminga J. October 2004 .*Response SurfaceMethodology.*CASOS Technical Report, CMU-ISRI-04-136.http://www.casos.cs.cmu.edu

[15]. Bas, D. & Boyacı, I. H. 2007.Modeling and optimization I: Usability of response surface methodology. *Journal of Food Engineering.* 78:836–845.

[16]. DOE++ .*Experiment Design & Analysis Reference.* 2014.

[17]. Da Silva, G.F., Gandolfi, P.H.K., Almeida, R.N., Lucas, A.M., Cassel, E. and Vargas, R.M.F. 2015.Analysis of supercritical fluid extraction of lycopodine using response surface methodology and process mathematical modeling. *Chemical engineering research and design*. 100:353-36.

[18]. Engineering Statistics Handbook. 2013. http://www.itl.nist.gov/div898/handbook/index.htm

[19]. Box, G. E. P., Hunter, W. G., and Hunter, J. S. 2005. Statistics for experimenters: An introduction to design, data analysis, and model building, 2nd Ed. New York: John Wiley & Sons.

[20]. Weisberg, S. 2005.*Applied Regression Analysis*.third Edition, John Wiley and Sons Inc., New Jersey.

[21]. "ANOVA Output" http://iiesl.utk.edu/Courses/IE340%20S07/Slides/Printing%20_ANOVA%20Output_.pdf

[22]. Adzamic, Z.,Adzamic, T.,Muzic, M. and Sertic-Bionda, K. 2 0 1 3.Optimization of the n-hexane isomerization process using response surface methodology. *Chemical engineering research and design*. 91:100–105.

[23]. Setiabudi, H.D., Jalil, A.A., Triwahyono, S., Kamarudin, N.H.N., Jusoh, R. 2013. Ir/Pt-HZSM5 for n-pentane isomerization: Effect of Si/Al ratio and reaction optimization by response surface methodology. *Chemical Engineering Journal*. 217:300–309.

[24]. Granato, D. and de Araujo Calado, V.M. 2014.*The use and importance of design of experiments (DOE) in process modelling in food science and technology,* Mathematical and Statistical Methods in Food Science and Technology, First Edition.Edited by Daniel Granato and Gaston Ares. John Wiley & Sons, Ltd